Fractographic Investigation on Solidification Crack in the Varestraint Test of Fully Austenitic Stainless Steel†

—Studies on Fractography of Welded Zone (III)—

Fukuhisa MATSUDA*, Hiroji NAKAGAWA, Seishiro OGATA*** and Seiji KATAYAMA******

Abstract

Fractographic study is made on hot cracks in fully austenitic stainless steel weld metal in order to elucidate the reasons why the weld metal is susceptible to hot cracks. Two types of hot cracks, that is, solidification cracks and ductility-dip cracks, are induced by the Trans-Varestraint test, and the crack surfaces are observed with a scanning electron microscope (SEM) and analyzed with an energy-dispersive type analyzer (EDX). SEM observation reveals that a feature of the solidification crack surface is gradually changing together with a drop in crack opening temperature. That is to say, the feature is dendritic Type D in higher temperature region and flat Type F in lower temperature region. The crack surface of Type D is supposed to have been covered with liquid phase at the moment of the crack-opening, judging from the morphology and the distribution of chromium on the crack surface. The crack surface of Type F is apparently flat, but it has many hollows where low melting inclusions are detected. The reason of occurrence of Type F is a decrease in liquid phase and an increase in grain boundary migration. The ductility of the weld metal is very low around Type D and gradually raised in Type F. Furthermore, the feature of ductility-dip crack surface and the behaviour of low melting inclusions enriched in sulphur or phosphorus on the crack surfaces are discussed.

1. Introduction

In recent years fractographic techniques have made many excellent contributions to elucidations of various fracture phenomena and mechanisms, but the applications of the techniques have generally been restricted to the fractures around and under the ambient temperature or at such a temperature, at the highest, as a creep fracture occurs.

On the other hand, hot cracks which are generally considered to be formed between the liquidus and the solidus temperature are great important problems together with cold cracks in the welding field. However, the hot cracks are backward in the fractographic analysis, except for the report of Honeycombe and Gooch[1], since the relation between a state of liquid phase at grain boundary at elevated temperatures and a feature of the crack surface has not been recognized in detail.

Therefore, in this report a detailed fractographic analysis with a scanning electron microscope (SEM) was conducted for a solidification crack in weld metal of a fully austenitic stainless steel which has an extremely high susceptibility to solidification cracking. As regards a method inducing the crack, the Trans-Varestraint test[2] was adopted, because the crack-opening temperature at each part of the crack can be obtained by measuring the temperature distribution in the weld metal along weld center owing to the instantaneous crack-opening. The effects of phosphorus and sulphur, which are well known to be harmful elements, on the crack surface were also investigated. Besides, the surface of a ductility-dip crack occurring in the weld metal was briefly analyzed.

2. Materials Used and Experimental Procedures

2.1 Materials Used

Materials used are 25Cr–20Ni type fully austenitic stainless steels. The chemical compositions are shown in **Table 1,** in which SUS 310S※ is a commercially available plate, and P1–P6 and S1–S3 are tentative plates similar to SUS 310S except for phosphorus or sulphur content respectively. In the series of P1–P6, the phosphorus content is varied from 0.003 to 0.092%. In the series of S1–S3, the sulphur content is varied from 0.004 to 0.062%. The plate thickness of each material is 3 millimeters.

† Received on April 11, 1978

* Professor
** Research Instructor
*** Former Graduate Student, now with Sumitomo Heavy Industries, LTD
**** Graduate Student, Osaka University

※ SUS 310S corresponds to AISI 310S. SUS is the designation for stainless steel in Japan Industrial Standard (JIS).

Table 1 Chemical compositions of materials used

Mark	Composition (wt.%)						
	C	Si	Mn	P	S	Cr	Ni
SUS 310S	0.08	0.94	1.58	0.022	0.007	24.7	20.4
P1	0.05	0.13	1.36	0.003	0.009	24.7	20.3
P2	0.05	0.54	1.33	0.013	0.012	25.1	19.9
P3	0.07	0.66	1.48	0.022	0.007	24.6	20.1
P4	0.07	0.56	1.41	0.032	0.013	24.7	19.9
P5	0.07	0.59	1.44	0.048	0.014	25.1	19.9
P6	0.08	0.59	1.43	0.092	0.014	25.1	20.0
S1	0.07	0.78	1.08	0.022	0.004	24.4	19.9
S2	0.07	0.73	1.05	0.022	0.017	24.5	19.9
S3	0.07	0.75	1.03	0.023	0.062	24.4	20.0

2.2 The Trans-Varestraint Test

The Trans-Varestraint test was performed to induce solidification cracks, while TIG-arc bead-on-plate welding without any filler metal was being carried out in conditions of 100A, 12–13V (DCSP), 150 mm/min. The temperature distribution of the weld metal was measured with a W/5%Re–26%Re thermocouples and a self-balancing pen-recorder. The detail of the test was the same as in the previous report.[3]

2.3 Observation of Crack Surface

The specimen, to which the augmented strain of 3.75% was applied by the Trans-Varestraint test, was fractured in a room temperature using a vice in order to expose the crack surface. Then, the crack surface was observed with a scanning electron microscope (SEM) and elements on the crack surface were analyzed with an energy dispersive-type analyser (EDX) or a wave dispersive-type analyser (EPMA) attached to the SEM.

3. Experimental Results and Discussions

3.1 Fractographic Features of Solidification Crack

The appearance of the weld metal of the commercial SUS 310S to which an augmented strain of 3.75% was applied by the Trans-Varestraint test is shown in **Fig. 1.** Two types of hot cracks, that is, solidification cracks and ductility-dip cracks, are observed in the weld metal[3]. Since the solidification crack is considered to be the more serious problem of these hot cracks[4], the solidification crack surface shall be first mentioned in detail.

The solidification crack surface in a low magnification is shown in **Fig. 2(a),** where the crack-opening temperature is lowered from the left to the right side. The crack surface shows a feature of intergranular fracture which is elongated unidirectionally due to the columnar growth, and the microscopic feature gradually changes from the higher temperature region to the lower temperature region. The detailed observation revealed that in the region at the highest temperature many fine protuberances were formed as in **Fig. 2(b),** whose size corresponded to that of the secondary arms of cellular dendrites observed on a polished and etched surface. Besides, tear-like protuberances shown in **Fig. 2(c)** were occasionally observed near the highest end, that is, near the liquidus temperature, which must also correspond to the liquid on the secondary dendrite arms. These regions shall be

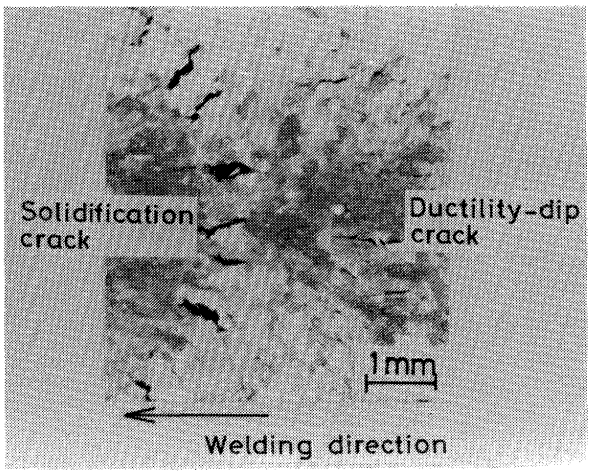

Fig. 1 General appearance of SUS 310S weld metal to which augmented-strain of 3.75% was applied with Trans-Varestraint test.

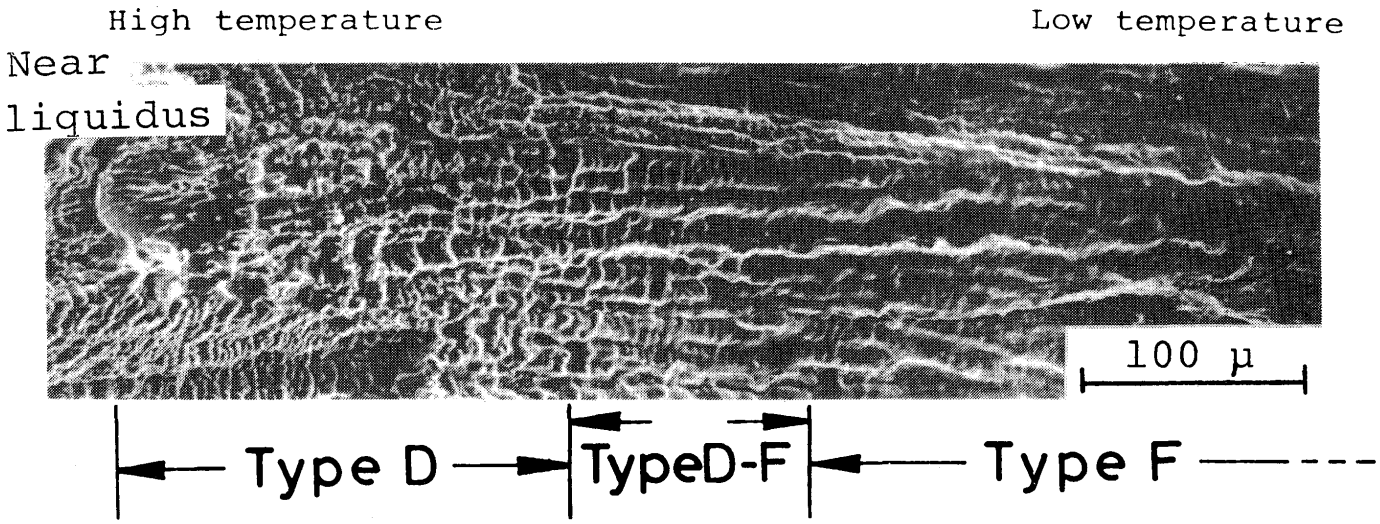

(a)

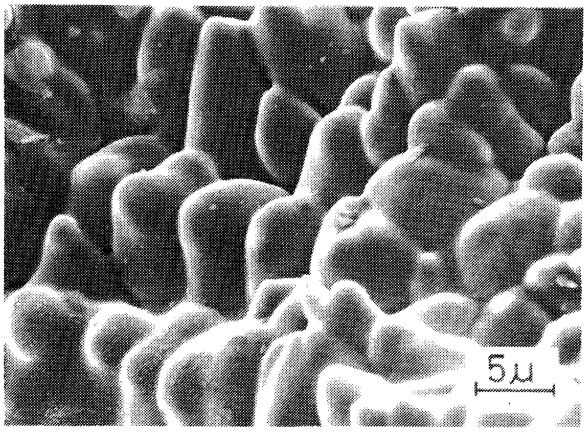

(b)

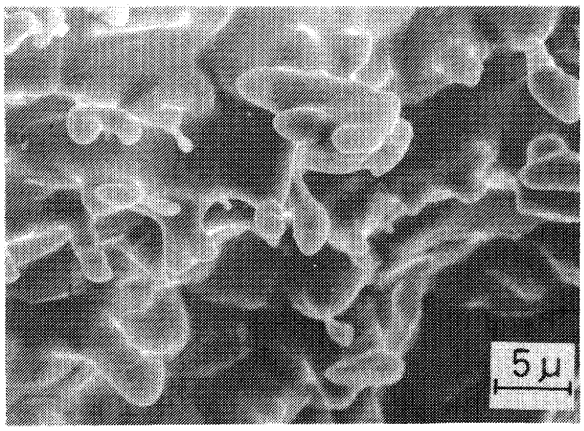

(c)

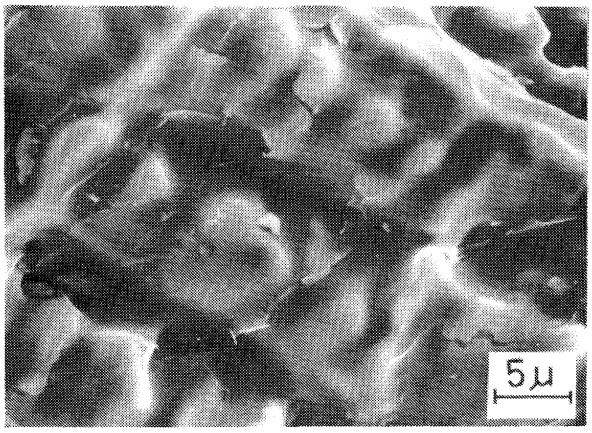

(d)

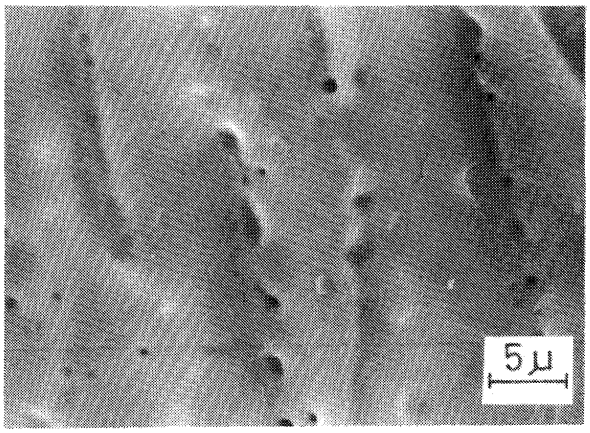

(e)

Fig. 2 Feature of solidification crack surface of SUS 310S weld metal
(a) general appearance in low magnification
(b) Type D in high magnification
(c) Type D_T in high magnification
(d) Type D-F in high magnification
(e) Type F in high magnification

hereafter named Type D, adopting the initial letter of "dendritic surface".

In the region at the medium temperature the protuberances of secondary arms gradually become obscure, and only grooves between primary dendrite arms parallel to the growing direction of the columnar crystal are somewhat noticeable. The crack surface is shown in a higher magnification in **Fig. 2(d).** This region shall be named Type D-F region, considering it a transient region from Type D to Type F next mentioned.

In the region at the lowest temperature the grooves between the primary dendrite arms also become obscure, and a flat surface becomes dominant. The crack surface in a higher magnification is shown in **Fig. 2(e).** This region shall be Type F region after the initial letter of "flat surface".

On the crack surface non-metallic inclusions were occasionally observed. Especially they were observed in a high probability in the hollows of the Type F region shown in Fig. 2(e). Examples of the inclusions in the hollows of the Type F region are shown in **Fig. 3.** The EDX and EPMA results on these in-

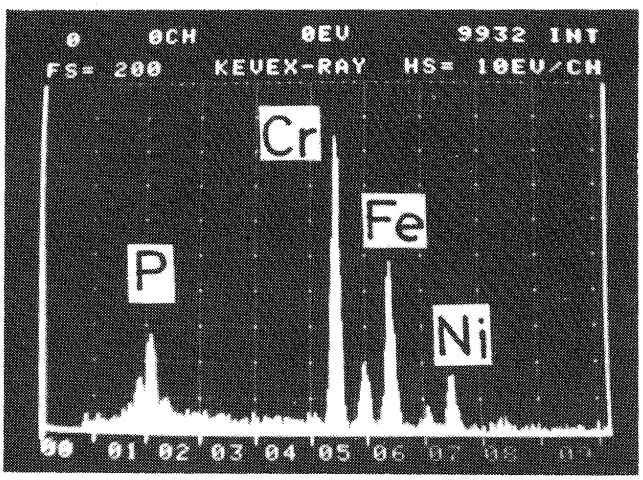

(a)

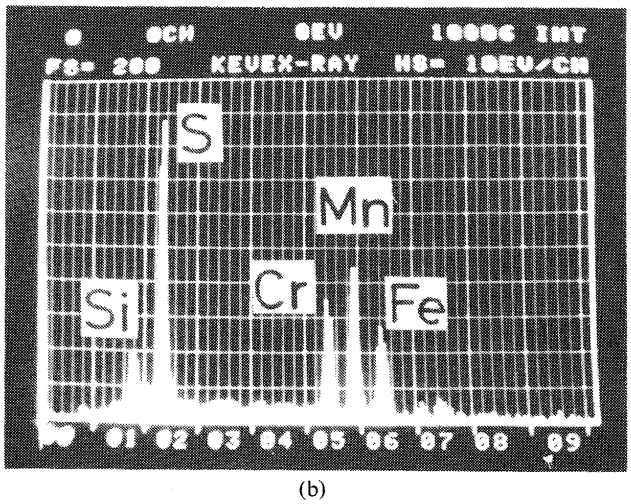

(b)

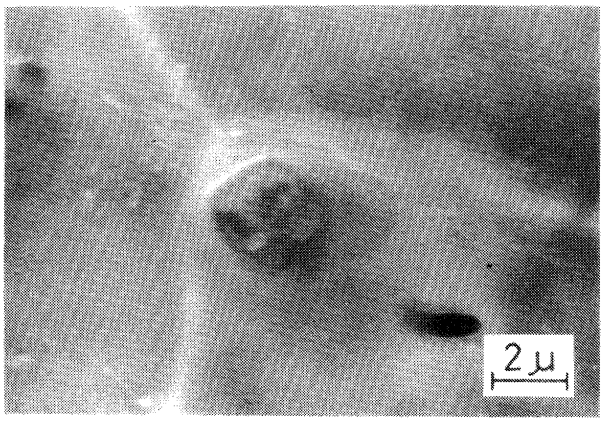

(a)

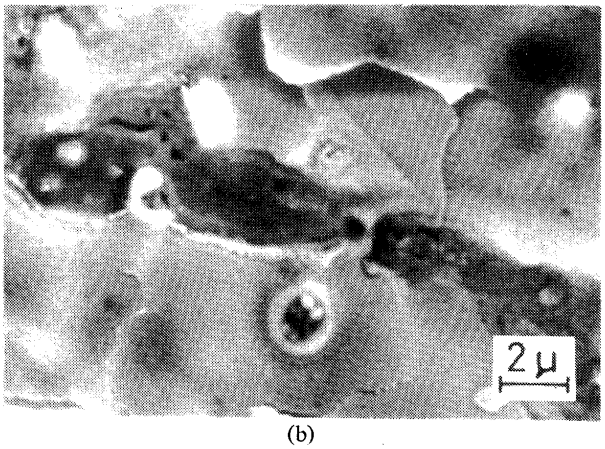

(b)

Fig. 3 Inclusions in hollows of Type F, material; SUS 310S.

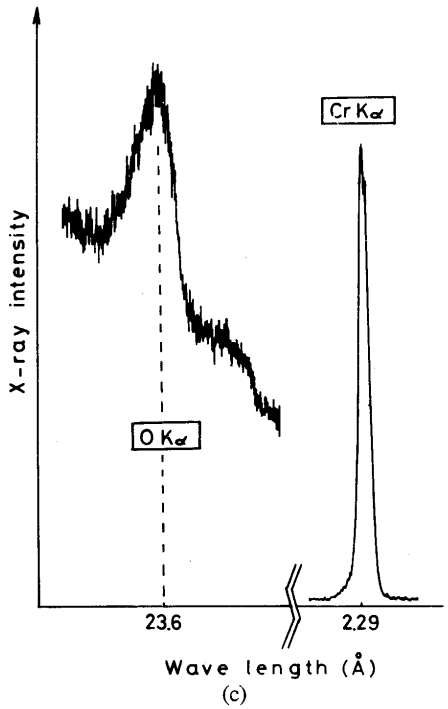

(c)

Fig. 4 Analyzed results on inclusions in hollows of Type F region with EDX or EPMA, material; SUS 310S.
(a) phosphide-type inclusion
(b) sulphide-type inclusion
(c) oxide-type inclusion

clusions, **Fig. 4,** revealed that they were phosphide-type inclusions as in Fig. 4(a), sulphide-type inclusions as in Fig. 4(b), or oxide-type inclusions containing a high Cr content as in Fig. 4(c).

3.2 Distribution of Chromium on Crack Surface and Grain Boundary Migration during Solidification

In SUS 310S chromium has a trend to segregate toward dendrite and grain boundaries during weld solidification[5]. Therefore, the distribution of chromium on the crack surface was investigated with EDX. For this purpose, the average X-ray counts of chromium detected from three parts, each dimension of which was $40 \times 30 \mu^2$ in area, were measured in each temperature region.

The result is shown in **Fig. 5.** The chromium count, which is nearly equal to the chromium contents, gradually increases from Type D toward Type D-F, and then gradually decreases in Type F. The count in the lowest temperature of Type F is nearly equal to that in an artificially fractured dimple region. The increase from Type D toward Type D-F can be explained from a viewpoint of the progress of the segregation during solidification. The gradual decrease in Type F, however, is inexplicable, since the diffusion

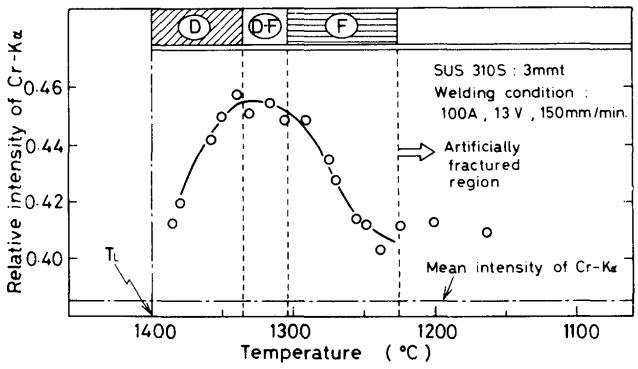

Fig. 5 Change in x-ray count of Cr-Kα on solidification crack surface, material; SUS 310S.

constant of chromium in the austenite is not so large as to eliminate the segregation during cooling after the solidification.

On the other hand, the microstructure quenched from the temperature corresponding to Type F during weld solidification was examined in **Fig. 6.** It showed that a grain boundary began to migrate during cooling even within the temperature range of Type F. Moreover, the result of a line analysis on Fig. 6 with EPMA, **Fig. 7** showed that chromium was still concentrated at the grain boundary of solidification but not at the migrated grain boundary during weld

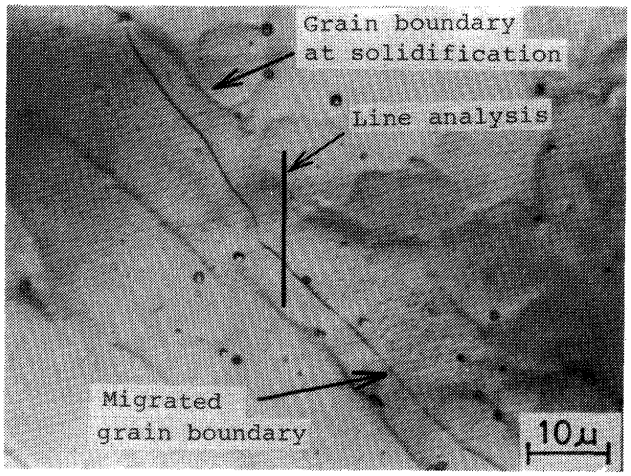

Fig. 6 Microstructure of weld metal showing grain boundary migration, material; SUS 310S.

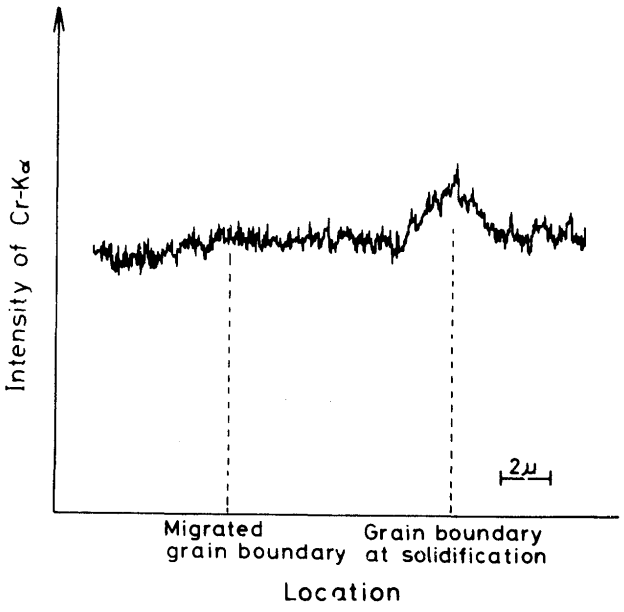

Fig. 7 Distribution of chromium content in weld metal, material; SUS 310S.

solidification. These results obtained in Figs. 5, 6 and 7 suggest that a grain boundary partly migrates even within the temperature range of Type F, and that the crack of Type F partly passes through the migrating grain boundary.

Therefore, the specimen quenched during welding was examined again in order to confirm the above-mentioned considerations. The microstructure of the part corresponding to the temperature of Type F at the moment of the water-quenching is shown in a higher magnification in **Fig. 8.** According to Fig. 8, the grain boundary partly begins to migrate, though the remaining parts of the grain boundary are stuck

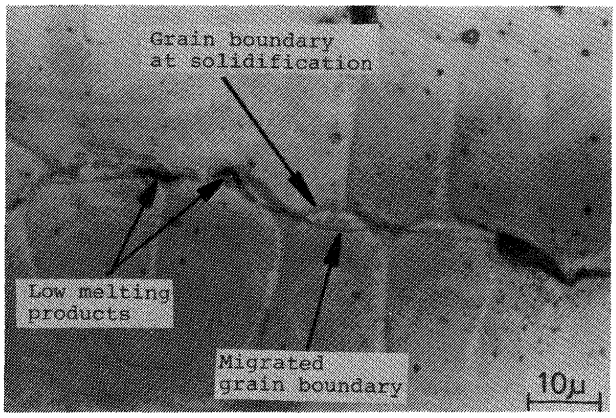

Fig. 8 Microstructure water-quenched from temperature in Type F region, material; SUS 310S.

to inclusions, which are generally supposed to be low melting liquid phase at the instance of the water-quenching. Then, the migration ratio of grain boundary was investigated from the liquidus temperature to about 1200°C and was defined as follows:

$$R_m \text{ (migration ratio of grain boundary)} = \frac{\Sigma a_i + 0.5\Sigma c_i}{35} \times 100\ (\%) \qquad (1)$$

where a_i and c_i are illustrated in **Fig. 9,** where the

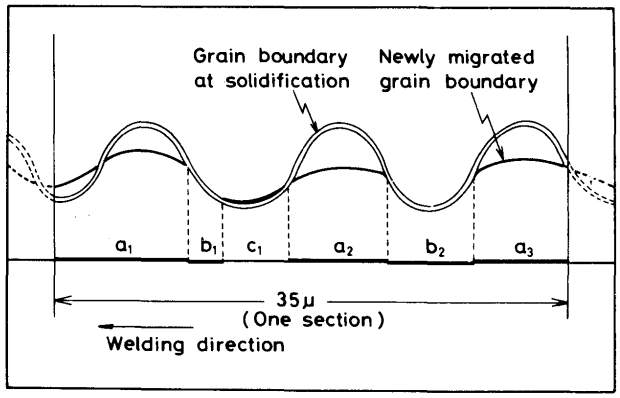

Fig. 9 Illustration of marks in equation (1)

migrated grain boundary and the original grain boundary at solidification are projected on a line parallel to the macroscopic direction of the grain boundaries. Now, a_i is a projected length of a migrated part, b_i is that of a remaining part, and c_i is that of an obscure part. The total length was selected to 35μ, considering errors owing to the temperature difference and to the stastical treatment of the data.

The results are shown in **Fig. 10,** where the migration ratio of grain boundary increases from 0 to 100 (%) in Type D-F and F. However, the feature of the crack surface of Type D-F, Fig. 2(d), gives the impression that liquid phase covers all over the crack surface and the grain boundary migration cannot

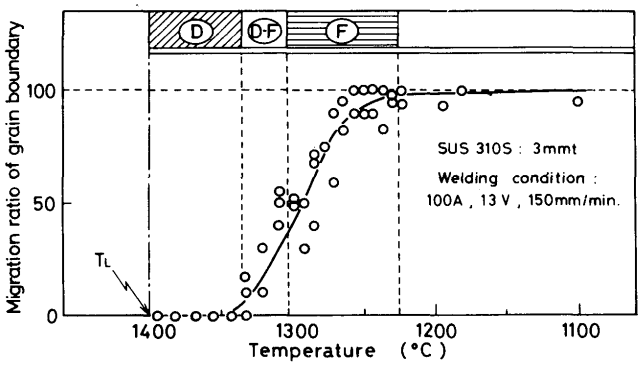

Fig. 10 Relation between migration ratio of grain boundary and temperature, T_L: Liquidus temperature, material; SUS 310S (water-quenched)

occur in Type D-F region. Therefore, an increase in the migration ratio in Type D-F may be due to the reason why the cooling rate by the water-quenching was not necessarily rapid sufficiently. Therefore, considering the effect of the water-quenching mentioned above, it may be said from Fig. 10 that the grain boundary gradually migrates in Type F together with the gradual decrease in the liquid phase at the original columnar solidification grain boundary.

Fig. 11 shows a microstructure containing an end

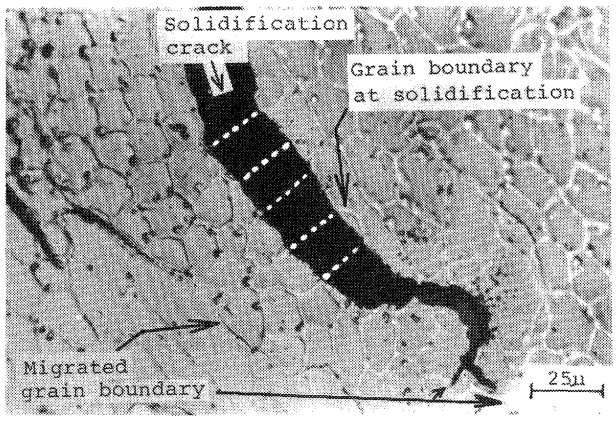

Fig. 11 Relation between migrated grain boundary and end of solidification crack in Type F, material; SUS 310S.

of the solidification crack corresponding to Type F, whose specimen was also water-quenched immediately after the crack was induced by the Trans-Varestraint test. The white dotted lines in the crack are drawn between the matching points of cellular dendrite

boundaries on the both crack surface. It is observed that the crack traverses the cellular dendrites except for inclusions and thus mainly passes through a migrated grain boundary.

Therefore, the reason why the X-ray counts of chromium gradually decreases in Type F as shown in Fig. 5 is that the crack passes through the migrating grain boundary together with the drop of the crack-opening temperature.

Now, it is interesting to know the relation between the type of the crack surface and the ductility of the weld metal. The ductility curve obtained by the Trans-Varestraint test is shown in **Fig. 12.** The

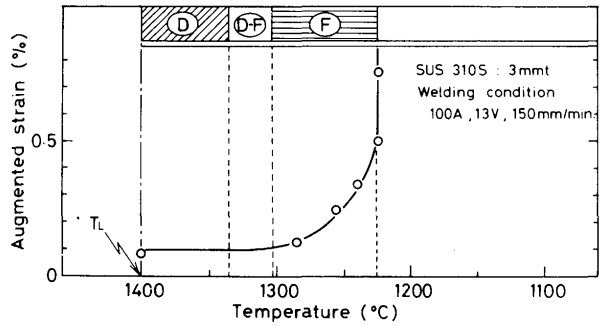

Fig. 12 Relation between temperature and ductility of weld metal obtained by Trans-Varestraint test, material; SUS 310S.

ductility, which is represented by the augmented-strain in the ordinate, is very low in Types D and D-F, and then gradually becomes high in Type F according to the temperature drop. Thus, the rise in the ductility corresponds to the decrease in the X-ray counts of chromium on the crack surface and to the increase in the migration ratio of the grain boundary.

3.3 Effect of Phosphorus on Crack Surface

In the previous section, it is yet unclear whether a low melting liquid phase really remains in Type F. On the other hand, it is reported[3] that phosphorus has an extremely detrimental effect on the solidification crack of SUS 310S and that M_3P type phosphides are formed in the grain boundary at solidification. Then, the effect of phosphorus content on the crack surface and the change in the morphology of phosphide on the crack surface were investigated.

The effect of phosphorus content on the ductility curve is shown in **Fig. 13.** The increase in phosphorus content extremely broadens the brittleness temperature range (BTR). Moreover, the lower limit temperatures of Types D, D-F and F are lowered by phosphorus as seen in **Fig. 14,** although that of Type F in phosphorus

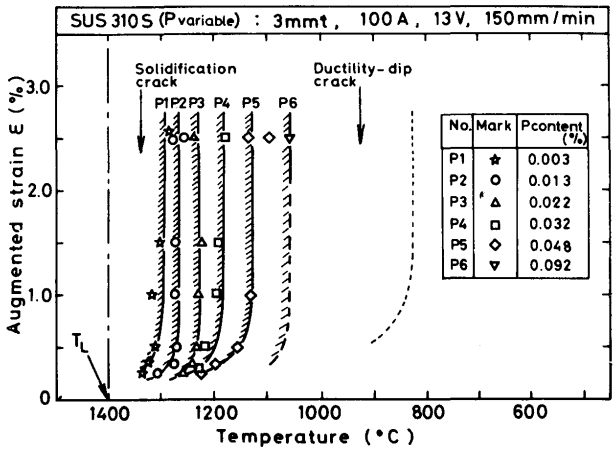

Fig. 13 Effect of phosphorus content on ductility curve of weld metal.

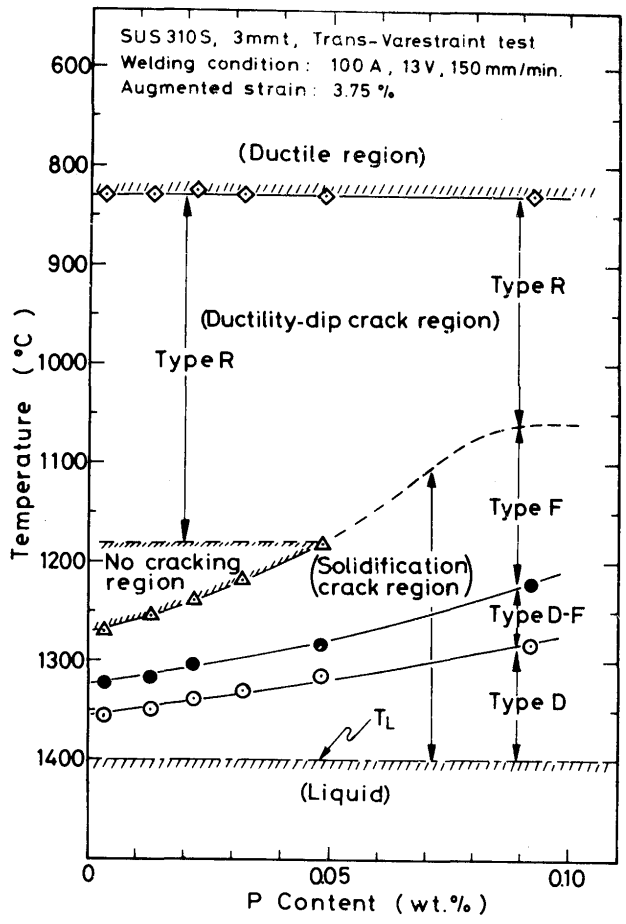

Fig. 14 Effect of phosphorus content on temperature ranges of Types D, D-F, F and R.

content above 0.048% is somewhat obscure due to the incorporation of Type F and Type R which represents the fracture surface of ductility-dip crack mentioned in 3.5.

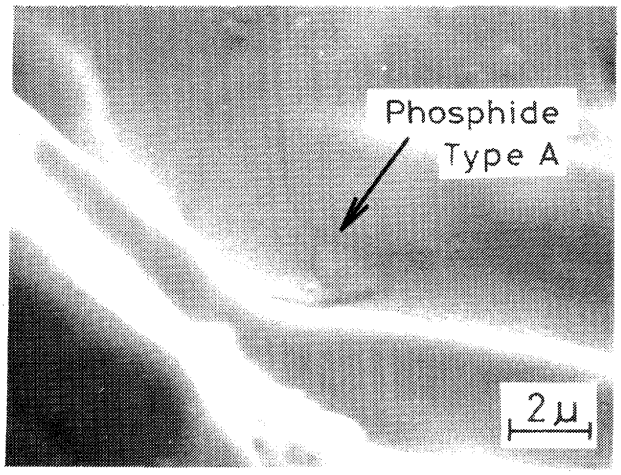

(a)

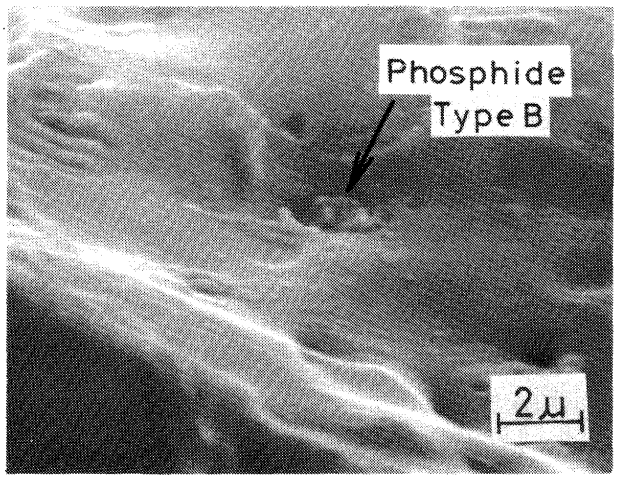

(b)

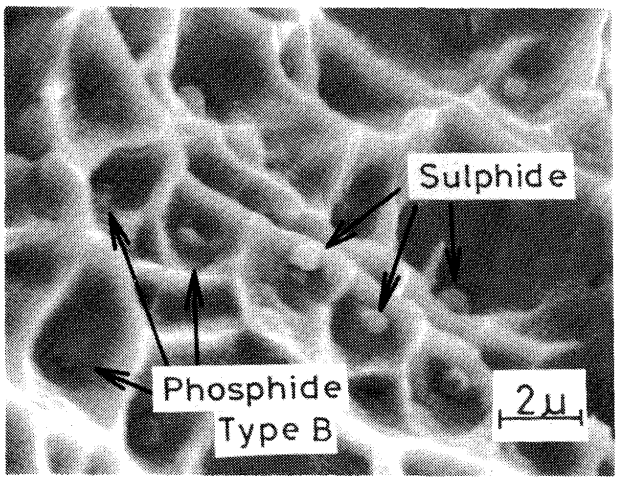

(c)

Fig. 15 Change in phosphide morphology on crack surface, material; P6 containing 0.092% phosphorus
(a) at 1280°C in Type D-F
(b) at 1040°C in Type R
(c) at room temperature in artificially fractured region

The change in the morphology of phosphides on the crack surface of the specimen P6 containing 0.092% phosphorus is shown in **Fig. 15.** The phosphides on the solidification crack give a tacky impression as seen in Fig. 15(a), which shall be named Type A, irrespective of Types D, D-F and F. On the other hand, the morphology of phosphides on the ductility-dip crack is generally granular as seen in Fig. 15(b), which shall be named Type B, and is identical with that of phosphides in dimples fractured compulsively at room temperature as seen in Fig. 15(c). Therefore, it is considered that the phosphides on the Type F crack have not yet completely solidified and thus remains as isolated liquid or liquid lakes at the instance of the crack-opening. Further this is confirmed by **Fig. 16,** which shows the effect of phosphorus content on the distribution of X-ray count of chromium on the crack surface. It is observed that the decrease in the X-ray count in Type F becomes gentle together with the increase in phosphorus content. This is considered to be due to that the higher the phosphorus content, the more liquid lakes remain in Type F and thus the migration ratio of grain boundary is lowered.

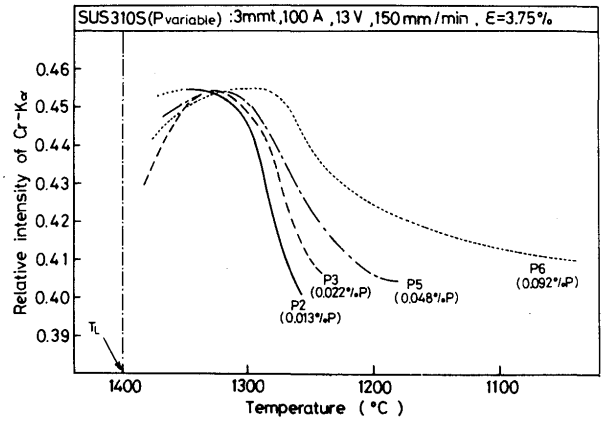

Fig. 16 Effect of phosphorus content on change in X-ray count of Cr-K_α on solidification crack surface.

3.4 Effect of Sulphur on Crack Surface

It is reported[3] that the detrimental effect of sulphur on the solidification crack of SUS 310S is small in spite of the formation of a large number of MnS type sulphides.

The effect of sulphur content on the ductility curve is shown in **Fig. 17.** The increase in sulphur content up to 0.062% hardly broadens the BTR.

The change in the morphology of sulphide on the crack surface of the specimen S3 containing 0.062%

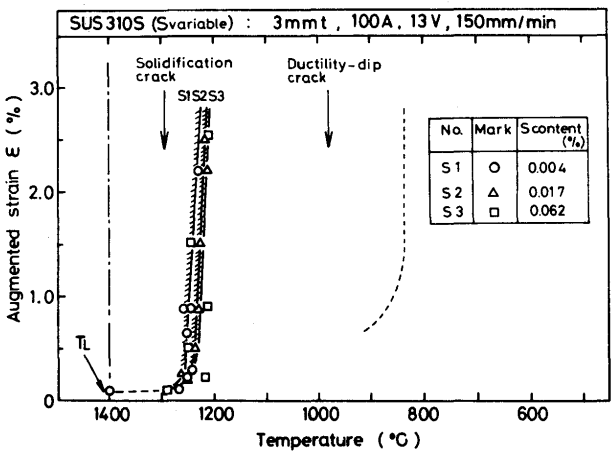

Fig. 17 Effect of sulphur content on ductility curve of weld metal.

sulphur is shown in **Fig. 18.** The sulphides on the Types D and D-F and the higher temperature part (above about 1300°C) of Type F give a tacky impression as seen in Fig. 18(a), which correspond to Type A. On the other hand, the morphology of sulphides on the remaining lower temperature of Type F and on the ductility-dip crack is rod-like, granular or grobular as seen in Fig. 18(b), which corresponds to Type B, and is identical with that in dimples of an artificially fractured region as seen in Fig. 18(c). Therefore, it is considered that the sulphides on the Type F below about 1300°C have already solidified at the instance of the crack-opening.

Judging from the results in the sections 3.3 and 3.4, it will be concluded that the liquid lakes mainly composed of liquid phosphides cause the broad Type F region in the commercial grade SUS 310S and/or impure SUS 310S.

3.5 Fractographic Feature of Ductility-dip Crack

As already mentioned in Fig. 1, the ductility-dip crack is formed together with solidification crack in the case of high augmented-strains. The temperature range within which the ductility-dip crack occurs is from about 1200 to 800°C, irrespective of the phosphorus content as seen in Fig. 14. The crack surface is shown in a low magnification in **Fig. 19(a),** which somewhat resembles the Type F. However, the observation in a higher magnification, **Fig. 19(b)** and **(c)**, revealed that there were no hollows as seen in Fig. 2(e) and that the crack surface gave a rough impression. This feature of the crack surface was named Type R, adopting the initial letter of "rough surface". Further EPMA analysis, **Fig. 20(a),** on dark and small hollows in Fig. 19(c) showed the

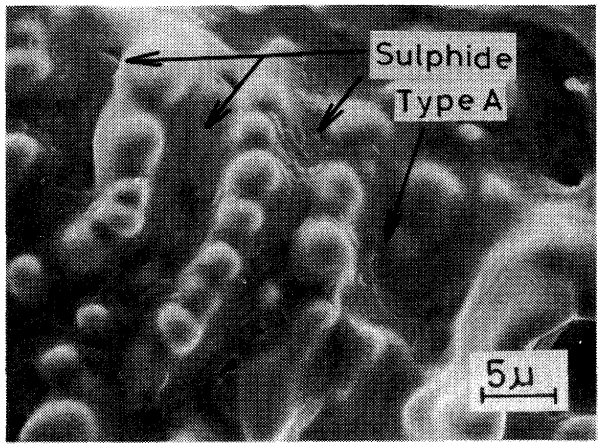

(a)

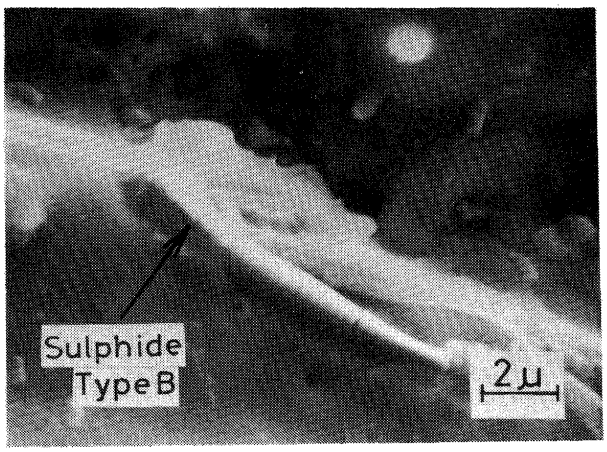

(b)

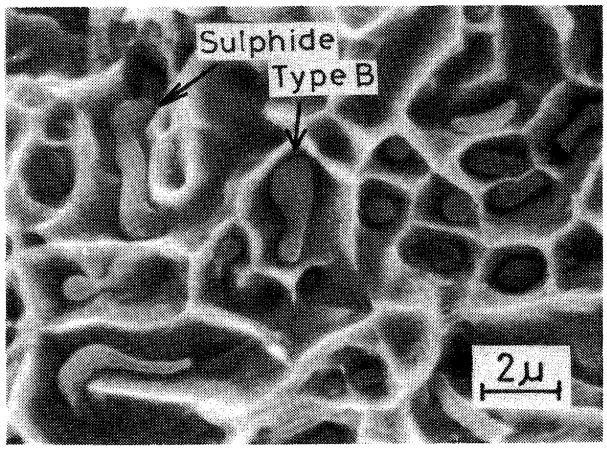

(c)

Fig. 18 Change in sulphide morphology on crack surface, material; S3 containing 0.062% sulphur
(a) at 1360°C in Type D
(b) at 1290°C in Type F
(c) at room temperature in artificially fractured region

existence of carbon and higher chromium than that of the other parts, **Fig. 20(b)**, and thus they are considered to be carbides.

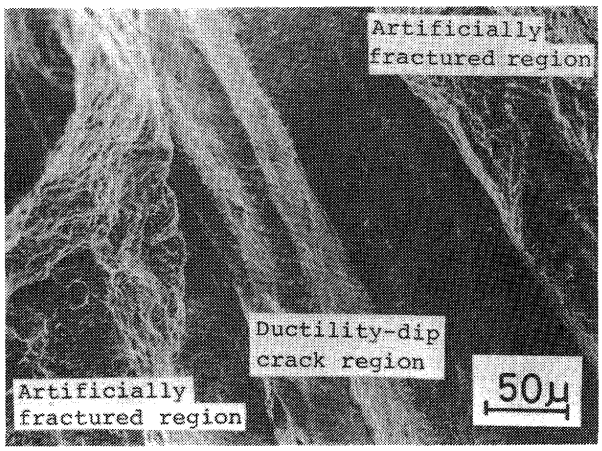

(a)

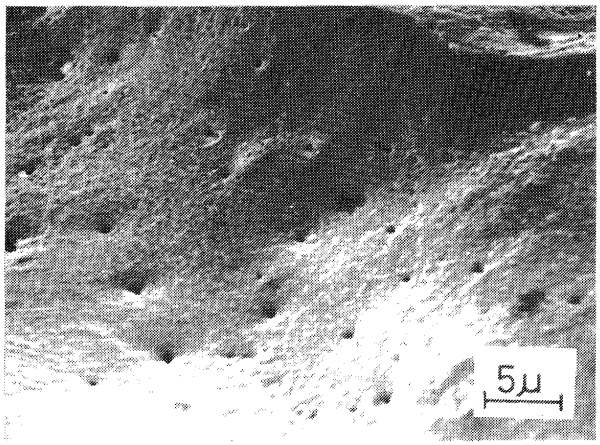

(b)

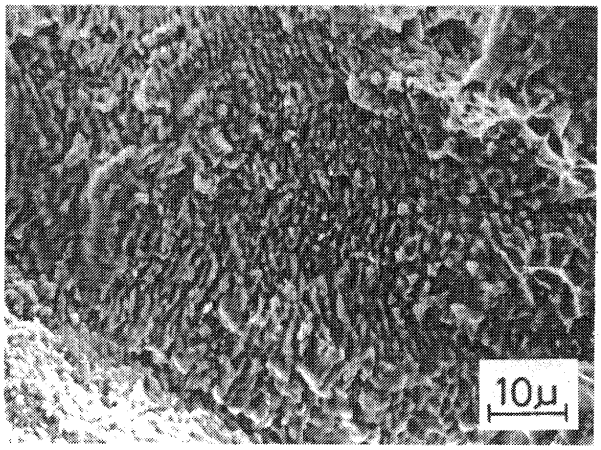

(c)

Fig. 19 Feature of ductility-dip crack surface of SUS 310S weld metal
(a) general appearance in low magnification
(b) example in high magnification
(c) example in high magnification

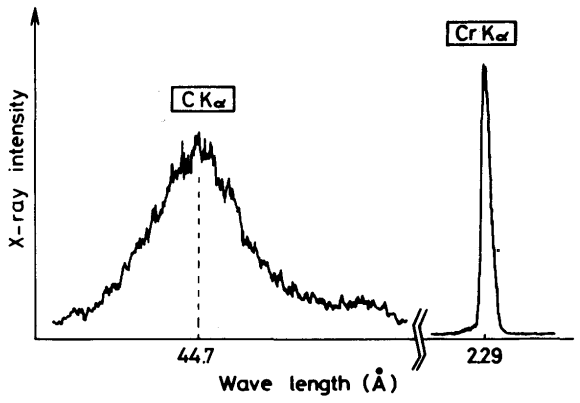

(a)

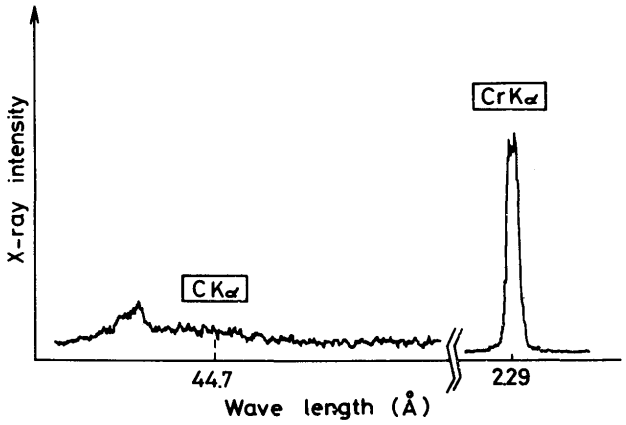

(b)

Fig. 20 EPMA result on small dark hollow of Type R (a) and matrix (b), material; SUS 310S.

3.6 Summary of Relation between State of Grain Boundary and Ductility

Above-mentioned results and discussions are summarized in **Fig. 21.** Fig. 21(a) is an illustration of a supposed solidification process of SUS 310S judging from metallographic examinations of water-quenched specimen during welding.[5] Fig. 21(b) shows qualitatively the change in liquid fraction at the grain boundary in Fig. 21(a) and the change in migration ratio of the grain boundary. The curve of the liquid fraction is drawn by reference to the results in Fig. 5. Fig. 21(c) shows qualitatively the ductility curve. By comparing these figures, it can be well understood the mutual relations. That is, in Types D and D-F the liquid phase covers all over the grain boundary and thus bridging of the solid phase can be hardly achieved. Thus the ductility of the weld metal is very low in Types D and D-F. In Type F the solid bridging starts and progresses together with

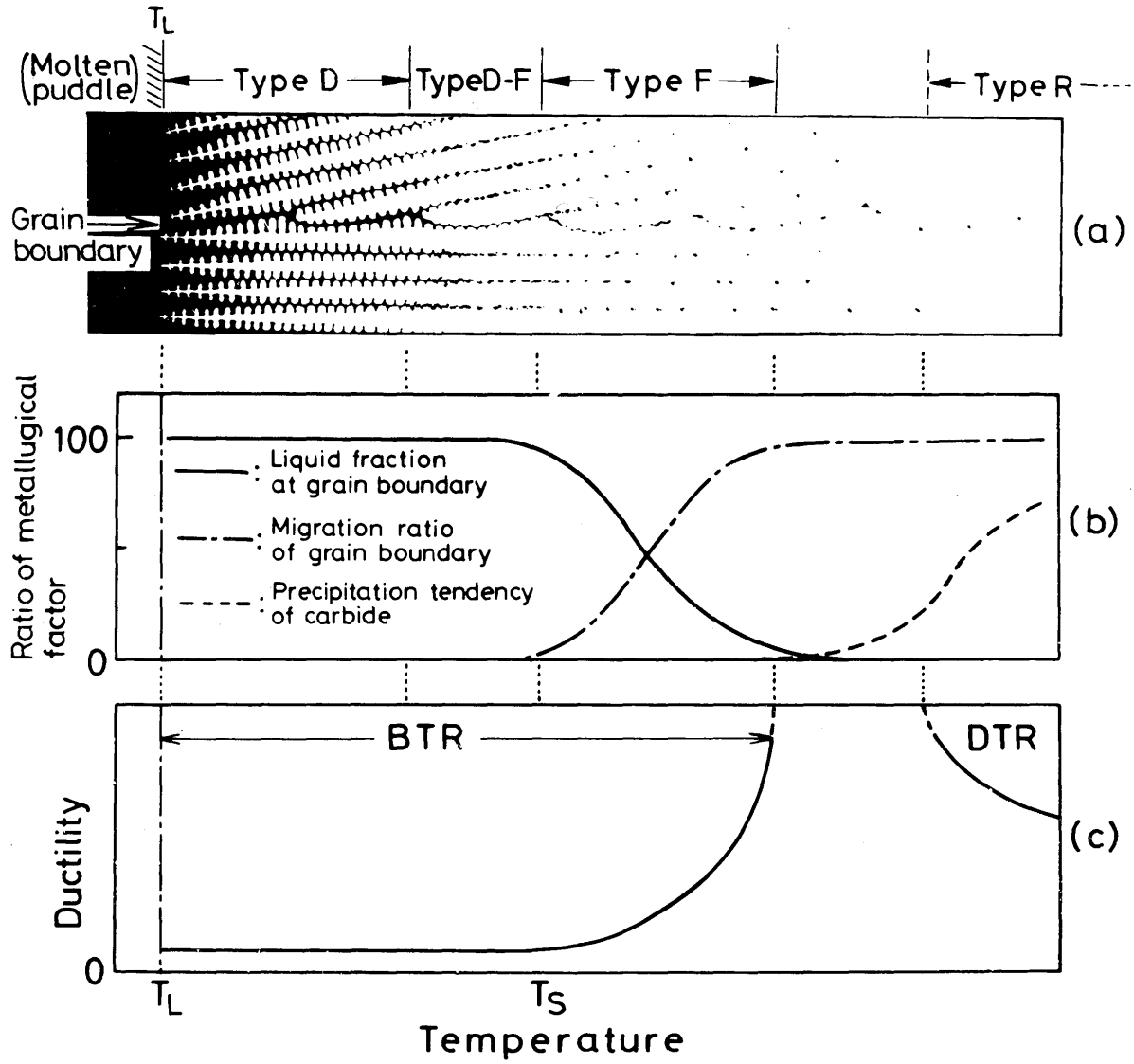

Fig. 21 Summary of correlation among solidification process, liquid fraction at grain boundary, and migration ratio of grain boundary and ductility of weld metal.

the temperature drop and the remaining liquid lakes gradually decrease. Moreover, in Type F the grain boundary migration occurs in the parts where the solid bridging has already finished, and the crack passes through the migrating grain boundary joining the liquid lakes enclosed in the solid. Thus the ductility in Type F gradually rises because the crack propagates in the solid owing to the increase in the solid bridging.

Furthermore, in the lower temperature region the precipitation of some carbides may cause the ductility-dip crack.

4. Conclusions

Main conclusions obtained are as follows:

1) The solidification crack surface has its characteristic appearance dependent on the crack-opening temperature. The crack surface in the highest temperature region has a feature of dendritic protuberances, and was thus named Type D. The crack surface in the lowest temperature region generally has a flat feature, although there are hollows in which non-metallic inclusions are observed, and it was named Type F. The crack surface in the medium temperature region has a transient feature from Type D to Type F, and

thus it was named Type D-F.

2) The ductility of the weld metal is very low in Types D and D-F, and gradually rises in Type F as the temperature drops.

3) The chromium content on the crack surface increases from Type D to Type D-F, but decreases gradually in Type F.

4) Grain boundary migration starts to occur in Type F, and the degree increases together with the temperature drop in Type F. The crack partly passes through the migrating grain boundary to join low melting inclusions.

5) Increase in phosphorus content lowers the lower temperature limits of Types D, D-F and F. The morphology of phosphides on the crack surface of Type F gives a tacky impression in contrast with granular morphology in dimples in an artificially fractured region. Consequently it is considered phosphides have not yet solidified in Type F.

6) Increase in sulphur content hardly influences the crack surface. The morphology of sulphides in Type F except for the highest region is identical with that of sulphides in dimples. Consequently, it is considered that the sulphide has already solidified in the lower temperature region of Type F.

7) From the above results in 2)–6), the cause of the formation of Types D, D-F and F and the relation between these features and the ductility can be considered as follows; In Types D and D-F dendrites are in the course of the growth and the liquid phase covers all over the grain boundary. In this case, the ductility is very low. In Type F solid bridging starts and progresses together with the temperature drop and the remaining liquid lakes gradually decrease. Moreover, in Type F grain boundary migration occurs in the parts where the solid bridging has already finished, and the crack passes through the migrated grain boundary joining the liquid lakes. Consequently, the ductility in Type F rises gradually owing to the solid bridging. The flat or smooth surface of Type F is formed because liquid phase decreases and the crack passes through the migrating grain boundary. The liquid lakes in Type F are mainly phosphide-type liquids.

8) Ductility-dip crack is also formed, and the crack surface in a low magnification somewhat resembles the Type F. However, the crack surface in a higher magnification gives a rough impression, and it was named Type R. Carbides are detected on the crack surface.

Acknowledgements

The authors wish to thank Mr. S. Saruwatari of Nippon Steel Corporation and Mr. K. Saito of Nippon Stainless Steel Corporation for their supplying materials used.

References

1) J. Honeycombe and T.G. Gooch: "Microcracking in Fully Austenitic Stainless Steel Weld Metal", Metal Const. & Brit. Weld. J., (1970) Sept., pp. 375–379.
2) T. Senda, F. Matsuda and G. Takano: "Studies on Solidification Crack Susceptibility for Weld Metals with Trans-Varestraint Test (2)", J. of JWS, Vol. 42 (1973) No. 1, pp. 48–56.
3) Y. Arata, F. Matsuda and S. Katayama: "Solidification Crack Susceptibility in Weld Metals of Fully Austenitic Stainless Steels (Report II)", Trans. JWRI, Vol. 6 (1977) No. 1, pp. 105–116.
4) Y. Arata, F. Matsuda, H. Nakagawa, S. Katayama and S. Ogata: "Solidification Crack Susceptibility in Weld Metals of Fully Austenitic Stainless Steels (Report III)", Trans. JWRI, Vol. 6 (1977) No. 2, pp. 198–206.
5) Y. Arata, F. Matsuda and S. Katayama: "Solidification Crack Susceptibility in Weld Metals of Fully Austenitic Stainless Steels (Report I)", Trans. JWRI, Vol. 5 (1976) No. 2, pp. 135–151.